Universal behaviors in the wrinkling transition of disordered membranes

O. Coquand, K. Essafi, J.-P. Kownacki, D. Mouhanna

Universal behaviors in the wrinkling transition of disordered membranes

O. Coquand,[1, 2, *] K. Essafi,[1, †] J.-P. Kownacki,[3, ‡] and D. Mouhanna[4, §]

[1]*Sorbonne Universités, CNRS, Laboratoire de Physique Théorique de la Matière Condensée, LPTMC, F-75005 Paris, France*
[2]*Institut für Materialphysik im Weltraum, Deutsches Zentrum für Luft- und Raumfahrt, Linder Höhe, 51147 Köln, Germany*
[3]*LPTM, CNRS UMR 8089-Université de Cergy-Pontoise,*
2 avenue Adolphe Chauvin, 95302 Cergy-Pontoise Cedex, France
[4]*Sorbonne Université, CNRS, Laboratoire de Physique Théorique de la Matière Condensée, LPTMC, F-75005 Paris, France*

The wrinkling transition experimentally identified by Mutz *et al.* [Phys. Rev. Lett. 67, 923 (1991)] and then thoroughly studied by Chaieb *et al.* [Phys. Rev. Lett. 96, 078101 (2006)] in partially polymerized lipid membranes is reconsidered. One shows that the features associated with this transition, notably the various scaling behaviors of the height-height correlation functions that have been observed, are qualitatively and quantitatively well described by a recent nonperturbative renormalization group approach to quenched disordered membranes by Coquand *et al.* [Phys. Rev E 97, 030102(R) (2018)]. As these behaviors are associated with fixed points of renormalization group transformations they are *universal* and should also be observed in, *e.g.*, defective graphene and graphene-like materials.

I. INTRODUCTION

A considerable activity has been devoted these last years to understanding both experimentally and theoretically the effects of disorder in membranes, mainly within the contexts of the current study of graphene and graphene-like materials on the one hand and, in a more distant past, of partially polymerized lipid membranes on the other hand. Indeed, the synthesis of graphene [1, 2] followed by the discovery of its outstanding mechanical, electronic, optical and thermal properties [3–6] has stimulated intensive researches aiming at understanding how the unavoidable presence of defects, vacancies, or adatoms would alter the physical properties of pristine compounds. Also, beyond the mere presence of native imperfections, the introduction of artificial defects, *e.g.* foreign adatoms or substitutional impurities, with the help of various processes – particle (electrons or ions) irradiation, chemical methods like oxidation or crystal growth – has given rise to the emergence of a whole defect engineering industry aiming at achieving new functionalities for these *topologically designed* graphene and graphene-like materials [7–10]. Among the numerous effects observed one finds: variation (increase or decrease) of electronic conductivity according to the size of the defects, increase of elasticity for moderate density of vacancies and decrease at higher density, decrease of thermal conductance, of fracture strength, enhancement of reactivity, appearance of ferromagnetism and so on [8–12]. As part of this defect engineering activity, a specific effort involving various experimental or numerical techniques – (low pressure) chemical vapor deposition [13], ion/electron irradiation [14–19] or molecular dynamic simulation [20–22] – has been made toward the design of defect-induced two-dimensional (2D) amorphous counterparts of graphene and graphene-like materials. A highlight of this activity is the achievement by electron irradiation of a step-by-step, atom-by-atom, crystal-to-glass

transition giving rise to a vacancy-amorphized graphene structure [13–15] similar to the continuous random network by Zachariasen [23]. Many characteristics of this transition have been determined: the onset of the defect-induced amorphization process, its temperature dependence, the structural response to vacancy insertion, the nature of the electronic density of states of the defective configurations [20], a transition in the fracture response from brittle to ductile when increasing vacancy concentration [24]; finally a careful analysis of the glassy-graphene structure in terms of a proliferation of nonhexagonal carbon rings has been performed [15, 22]. However we emphasize that the very nature of this glass transition is still unclear. Moreover there has been, up to now, neither within this last context nor within the more general one of the investigation of defective graphene and graphene-like materials, no characterization of a quantitative change between – still putative – ordered and disordered phases and *a fortiori* no indication of universal behaviors associated with them.

In marked contrast with this situation, in a very different context, recent investigations of partially polymerized lipid membranes by Chaieb *et al.*[25], following the pioneering work of Mutz *et al.*[26], have led to identify a remarkable folding-transition while varying the degree of polymerization. More precisely these authors have shown that, upon cooling below the chain melting temperature, partially polymerized phospholipid vesicles undergo a transition from a relatively smooth structure, at high polymerization, to a *wrinkled* structure, at low polymerization, characterized by randomly frozen normals. This has led them to suggest that this transition would be the counterpart of the spin-glass transition occurring in disordered spin systems [26, 27]. Chaieb *et al.* [25], by considering the height-height correlation functions, have been able to characterize quantitatively the various phases as well as the *wrinkling* transition separating them. However, despite the large amount of theo-

retical work oriented towards understanding the physics of disordered membranes, no theoretical explanation has been given so far on the grounds of these results [27–38].

In this article, we show that a recent nonperturbative renormaliation group (NPRG) study, performed by the present authors [39], of the effective theory used to study both curvature and metric disorders perfectly accounts for this situation. In a first part, we recall the experimental status of wrinkled partially polymerized membranes. In a second part, we lay out the unusually unsettled state of the theoretical situation. Finally, in a third part, performing an analysis of the long-distance morphology of membranes at and in the vicinity of the wrinkling transition, we show how the NPRG approach reproduces the experimental outputs. Finally we conclude, stressing the consequences of our analysis for the physics of graphene and graphene-like materials and claiming, in particular, that the behaviors observed in partially polymerized lipid membranes should also be observed in these materials.

II. WRINKLING TRANSITION IN PARTIALLY POLYMERIZED MEMBRANES

The identification of a wrinkling transition in partially polymerized membranes goes back to the work of Sackman *et al.* [40] on mixture of diacetylenic phospholipids and dimyristoylphosphatidylcholine, followed by those of Mutz *et al.* [26] and Chaieb *et al.* [25] on diacetylenic phospholipids [1,2-bis(10,12-tricosadiynoyl)-*sn*-glycero-3-phosphocholine], who have taken advantage of the fact that, upon a chemical or photochemical process, notably ultraviolet (UV) irradiation, these compounds polymerize. In the case considered in [26] the polymerizable phospholipids are first prepared as giant vesicles and then cooled below the chain melting temperature $T_m \simeq 40°C$ where they form tubular structures that are then partially polymerized by UV irradiation. The membranes are then reheated above T_m where they reform spherical vesicles provided the degree of polymerization does not exceed the percolation threshold located around 40 %. These vesicles, of typical size ranging from 0.3 to 40 μm, are then cooled down to $T_w \simeq 18 - 22°C$ where they undergo a spontaneous, reversible, phase transition from a relatively smooth structure to a *wrinkled*, highly convoluted, rigid one displaying locally high spontaneous curvature. This observation has led Mutz *et al.* [26] to conjecture that this state of affairs should be well described by a theory of polymerized membranes submitted to quenched curvature disorder. The outcomes of this experiment have been made more quantitative by Chaieb *et al.* [25, 41–43] who have studied the transition by various techniques. Small angle neutron scattering has been used to investigate the local structure, giving access to the fractal dimension while environmental scanning electron microscopy has

been employed for the study of the surface topography at mesoscopic scale [25, 41–43]. Finally a tapping-mode atomic force microscope has provided information on the mean-square fluctuations of the surface height $h(\mathbf{x})$ at a point $\mathbf{x} = (x_1, x_2)$, relative to the mean surface height, $\langle (h(\mathbf{x}) - h(\mathbf{0}))^2 \rangle$, and its Fourier transform, the power spectrum $P(k)$ [25]. This last quantity has been found to display a remarkable power-law behavior in the range $0.1 - 100 \ \mu m^{-1}$: $P(k) \sim k^{-\gamma}$ where the power exponent γ [64] is directly related to the roughness exponent ζ by: $\gamma = 1 + 2\zeta$. Three clear distinct regimes have been observed [25] as the degree of polymerization ϕ is varied, see Fig.1. At low polymerization, typically for $\phi < 30\%$, the surface of the vesicles presents – at large scales – large deformations, creases, of order of the vesicle size (500 nm) typical of a wrinkled state. In this case one finds [25]: $\gamma = 2.9 \pm 0.1$ corresponding to $\zeta = 0.95 \pm 0.05$. At high polymerization, typically between 32 and 40% the vesicles are regular at large scales and the creases are less pronounced (of order 20 nm) and one has [25] : $\gamma = 2 \pm 0.06$ and $\zeta = 0.5 \pm 0.03$. Finally, for ϕ in the intermediary region $30\% \leq \phi < 32\%$ a transition occurs and the vesicles display the morphology of a crumpled elastic sheet with $\gamma = 2.51 \pm 0.03$ and $\zeta = 0.75 \pm 0.02$ [25].
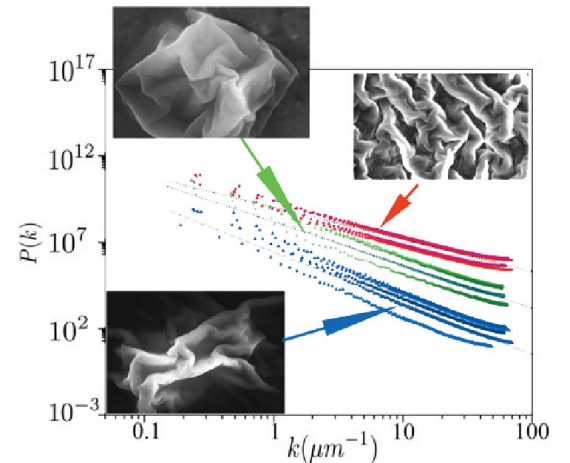

FIG. 1: The three scaling behaviors of the power spectrum $P(k)$ as function of k for various degrees of polymerization ϕ of the membrane. From top to bottom: $\phi = 40\%$, $\phi = 30\%$ and $\phi = 9\%$ and the corresponding membrane configurations. From Chaieb *et al.* [25] with permission.

III. THEORETICAL CONTEXT

Early investigations of the wrinkling transition by Mutz *et al.* [26] have triggered an impressive series of theoretical works aiming to understand the effects of quenched disorder contributions in the seminal model of

Nelson and Peliti [44] used to describe the flat phase of disorder-free polymerized membranes [45–55]. This series has been initiated by Nelson and Radzihovsky [28, 29] who have mainly investigated the effects of impurity-induced disorder in the preferred metric tensor. They have in particular shown that, below the dimension $D = 4$ of the membrane, the flat phase of disorder-free membranes remains stable at any finite temperature T but should be destabilized at vanishing T for any amount of disorder due to a softening of the bending rigidity, making possible the emergence of a spin-glass behavior. This scenario has been strengthened by the work of Radzihovsky and Le Doussal [30] who, studying the limit of large embedding dimension d of the model, have identified an instability of the flat phase toward a spin-glass-like phase characterized by a nonvanishing Edwards-Anderson order parameter [56]. At the same time Morse *et al.* [57, 58], extending the work done in [28, 29], have considered the role of both curvature and metric quenched disorders. Using a perturbative, weak-coupling, $\epsilon = 4 - D$ expansion, they have shown that the curvature disorder gives rise to a new fixed point at $T = 0$, *stable* with respect to randomness but *unstable* with respect to the temperature. These works have been followed by an intensive search for various kinds, *i.e.* flat or crumpled, of glassy phases by means of mean-field approximations involving either short-range [27, 30–35] or long-range disorders [36, 37] (see also [38] for a review) that have led to predict that, at sufficiently strong disorder, the flat phase could be even unstable at any finite temperature toward a glassy phase that would correspond to the experimentally observed wrinkled phase. However, we would like here to emphasize several facts. The first one is that these last approaches, based on mean-field, large d, computations, should be considered with great caution when their conclusions are extended in the finite d case, particularly when they involve a breakdown of the symmetry between replica used to perform the average over disorder. Second, none of the approaches – involving $1/d$ or $\epsilon = 4 - D$ expansions – has been carried out at next-to-leading order, where new physics could emerge. Finally, none of them has produced quantitative predictions or explanations as for the results of Chaieb *et al.* [25].

IV. NPRG ANALYSIS

Recently however, following previous works on disorder-free polymerized membranes [50, 52, 55, 59–61] the present authors [39] have performed a NPRG approach of the model considered within a perturbative framework by Morse *et al.* [57, 58] and whose action

is given by

$$S[\boldsymbol{R}] = \int \mathrm{d}^D x \left\{ \frac{\kappa}{2} \left(\partial_i^2 \boldsymbol{R}(\boldsymbol{x}) \right)^2 + \frac{\lambda}{2} u_{ii}(\boldsymbol{x})^2 + \mu\, u_{ij}(\boldsymbol{x})^2 \right.$$
$$\left. - \boldsymbol{c}(\boldsymbol{x}) . \partial_i^2 \boldsymbol{R}(\boldsymbol{x}) - \sigma_{ij}(\boldsymbol{x})\, u_{ij}(\boldsymbol{x}) \right\} . \tag{1}$$

In this action $\boldsymbol{R}(\boldsymbol{x})$ is a d-dimensional vector field parametrizing, in the embedding space, the points $\boldsymbol{x} \equiv x_i$, $i = 1 \ldots D$ of D-dimensional membrane while u_{ij} is the strain tensor that represents the fluctuations around a flat reference configuration $\mathbf{R}^0$: $u_{ij} = \frac{1}{2}(\partial_i \boldsymbol{R} . \partial_j \boldsymbol{R} - \partial_i \boldsymbol{R}^0 . \partial_j \boldsymbol{R}^0)$ with [65]

$$\boldsymbol{R}^0 = [\langle \boldsymbol{R}(\boldsymbol{x}) \rangle] = x_i \boldsymbol{e}_i \tag{2}$$

where $\langle \ldots \rangle$ and $[\ldots]$ denote thermal and disorder averages respectively. In Eq.(2) the $\boldsymbol{e}_i$ form an orthonormal set of D vectors. The coupling constants κ and (λ, μ) represent respectively the bending rigidity and the Lamé coefficients. The action (1) includes curvature and metric disorder contributions induced by two random fields $\boldsymbol{c}(\boldsymbol{x})$ and $\sigma_{ij}(\boldsymbol{x})$ that couple to the curvature and strain tensor respectively. They are considered here as short-range, gaussian fields with [57, 58]

$$[c_i(\boldsymbol{x})\, c_j(\boldsymbol{x}')] = \Delta_\kappa\, \delta_{ij}\, \delta^{(D)}(\boldsymbol{x} - \boldsymbol{x}')$$

$$\left[\sigma_{ij}(\boldsymbol{x})\, \sigma_{kl}(\boldsymbol{x}')\right] = (\Delta_\lambda \delta_{ij}\delta_{kl} + 2\Delta_\mu I_{ijkl})\, \delta^{(D)}(\boldsymbol{x} - \boldsymbol{x}') \tag{3}$$

where $I_{ijkl} = \frac{1}{2}(\delta_{ik}\delta_{jl} + \delta_{il}\delta_{jk})$, with $i, j, k, l = 1 \ldots D$ where Δ_κ and $(\Delta_\mu, \Delta_\lambda + (2/D)\Delta_\mu)$ are positive coupling constants associated with curvature and metric disorders. Note finally that the ansatz (1), albeit reduced to four powers of the fields and field derivatives, is expected to lead to predictions not altered by higher orders, as this happens quite remarkably in the disorder-free case [52, 55, 60] and as this is strongly suggested by the very weak sensitivity of our results with the changes of renormalization group (RG) process – see below.

The RG equations corresponding to action (1) have been derived first perturbatively in [57, 58] and then within a NPRG approach in [39]. Within this latter approach the RG equations have revealed that there exist, in the space of coupling constants, not only *two*, as found by Morse *et al.* [57, 58] but actually *three* nontrivial fixed points: the usual finite-T, vanishing-disorder fixed point P_4 associated with disorder-free membranes [47]; a vanishing-T, finite-disorder fixed point P_5 identified for the first time in [57, 58]; finally a finite-T_c, finite-disorder fixed point P_c found in [39], missed within previous approaches, *unstable* with respect to T, thus associated with a second-order phase transition and making the $T = 0$ fixed point *fully attractive* provided $T < T_c$. The consequences of these facts are twofold: 1) a whole "glassy phase" associated with the $T = 0$ fixed point is predicted in agreement with the wrinkled phase observed in [25, 26]

and 2) three distinct universal scaling behaviors are expected, in agreement with the observations of Chaieb *et al.* [25]. The subsequent analysis shows, moreover, the *quantitative* agreement between the scaling behaviors predicted and those observed. The quantity to consider is the roughness exponent ζ. Let us recall how this quantity is defined in a field-theoretical context. Let us decompose $\boldsymbol{R}(\boldsymbol{x})$ around the flat phase configuration $\boldsymbol{R}^0(\boldsymbol{x})$ according to $\boldsymbol{R}(\boldsymbol{x}) = \boldsymbol{R}^0(\boldsymbol{x}) + \boldsymbol{u}(\boldsymbol{x}) + \boldsymbol{h}(\boldsymbol{x})$ where $\boldsymbol{u}(\boldsymbol{x})$ and $\boldsymbol{h}(\boldsymbol{x})$ are respectively the in-plane – phonon – and out-of-plane – flexuron, – degrees of freedom parametrizing the fluctuations around $\boldsymbol{R}^0(\boldsymbol{x})$. Writing $\delta\boldsymbol{h}(\boldsymbol{x}) = \boldsymbol{h}(\boldsymbol{x}) - \langle\boldsymbol{h}(\boldsymbol{x})\rangle$ one defines the connected and disconnected correlation functions of the $\boldsymbol{h}$ field by:

$$\left[\langle(\boldsymbol{h}(\boldsymbol{x}) - \boldsymbol{h}(\boldsymbol{0}))^2\rangle\right] = T\chi(\boldsymbol{x}) + C(\boldsymbol{x})$$

where $T\chi(\boldsymbol{x}) = \left[\langle(\delta\boldsymbol{h}(\boldsymbol{x}) - \delta\boldsymbol{h}(\boldsymbol{0}))^2\rangle\right]$ and $C(\boldsymbol{x}) = \left[\langle\boldsymbol{h}(\boldsymbol{x}) - \boldsymbol{h}(\boldsymbol{0})\rangle^2\right]$ that, as usual, respectively measure the thermal and disorder fluctuations. The long-distance behavior of these correlation functions is typically given by: $T\chi(\boldsymbol{x}) \sim |\boldsymbol{x}|^{2\zeta}$ and $C(\boldsymbol{x}) \sim |\boldsymbol{x}|^{2\zeta'}$ that define two roughness exponents ζ and ζ'. In the same way correlation functions are defined for the phonon field with two roughness exponents ζ_u and ζ_u'. They are related to the previous ones by: $\zeta_u = 2\zeta - 1$ and $\zeta_u' = 2\zeta' - 1$. Similarly, in momentum space, writing $\delta\boldsymbol{h}(\boldsymbol{q}) = \boldsymbol{h}(\boldsymbol{q}) - \langle\boldsymbol{h}(\boldsymbol{q})\rangle$, one defines:

$$G_{hh}(\boldsymbol{q}) = \left[\langle\boldsymbol{h}(\boldsymbol{q})\boldsymbol{h}(-\boldsymbol{q})\rangle\right] = T\chi(\boldsymbol{q}) + C(\boldsymbol{q}) \qquad (4)$$

where $T\chi(\boldsymbol{q}) = \left[\langle\delta\boldsymbol{h}(\boldsymbol{q})\delta\boldsymbol{h}(-\boldsymbol{q})\rangle\right]$ and $C(\boldsymbol{q}) = \left[\langle\boldsymbol{h}(\boldsymbol{q})\rangle\langle\boldsymbol{h}(-\boldsymbol{q})\rangle\right]$ that behave, at low momenta, as $\chi(\boldsymbol{q}) \sim q^{-(4-\eta)}$ and $C(\boldsymbol{q}) \sim q^{-(4-\eta')}$ where η and η' are the anomalous dimensions evaluated at the fixed points of the RG equations. As a consequence of expression (4) the scaling behavior expected for the height-height correlation function $G_{hh}(\boldsymbol{q})$ is determined by the relative value of η and η' together with the position of the fixed point: at finite or at vanishing T [66]. These exponents are related to the roughness exponents by: $\zeta = \frac{1}{2}(4 - D - \eta)$ and $\zeta' = \frac{1}{2}(4 - D - \eta')$ and to the power exponent $\gamma = 5 - D - \eta$ or $\gamma = 5 - D - \eta'$ depending on the exponent – η or η' – that controls the long-distance behavior.

At the fully *attractive*, vanishing-T, finite-disorder fixed point P_5 we find, by improving the results of [39], $\eta_5 = 0.448(2)$ and $\eta_5' = 0.275(2)$ [67]. This is in contrast with both [57, 58] and [38] where $\eta_5 = \eta_5'$ so that P_5 was found to correspond to a *marginal* – in fact marginally unstable – fixed point. As a consequence we find a roughness exponent $\zeta_5' = 0.862(1)$ that, according to (4) and the scaling laws of $\chi(\boldsymbol{q})$ and $C(\boldsymbol{q})$, controls the long-distance behavior of the height-height correlation function $G_{hh}(\boldsymbol{q})$. This corresponds to a power exponent $\gamma_5 = 2.725(2)$. This value is very close to that found in [25] at low polymerization – for ϕ in [10%; 30%] – and lies in the range [2.80, 2.92], see Fig.2. As done

in [25] we exclude the data point at lowest polymerization (corresponding to $\gamma = 3$ in Fig.2), which does not belong to the plateau identified for ϕ in [10%; 30%]. Note that such a value would correspond to the expected value for a *fluid* membrane, which could be a hint that below $\phi = 10\%$, partially polymerized lipid membranes do not behave as polymerized membranes anymore. At the *stable*, finite-T, finite-disorder fixed point P_4, we find $\eta_4 = \eta_4'/2 = 0.849(3)$ (see [39, 50, 60] and also [5] for a review of other approaches) that corresponds to $\zeta_4 = 0.575(2)$ and $\gamma_4 = 2.151(3)$. As seen in Fig.2 this is again in good agreement with the results found in [25] at high polymerization with a value of γ that saturates at 2. This value corresponds to the case of disorder-free polymerized membranes. It is in agreement with that obtained by Locatelli *et al.* [62] who have found $\zeta = 0.54 \pm 0.02$ by means of low energy electron diffraction on free-standing graphene sheet. Finally, at the finite-disorder, finite-T, *critical*, fixed point P_c found in [39] we get $\eta_c = \eta_c' = 0.490(2)$ that corresponds to $\zeta_c = 0.755(1)$ and $\gamma_c = 2.510(2)$ that is in very good agreement with the value $\gamma = 2.51$ found by Chaieb *et al.* [25] at critical polymerization, see Fig.2.
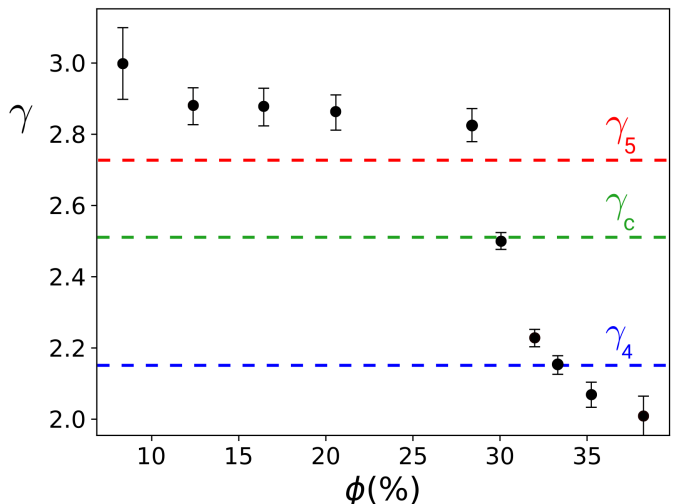

FIG. 2: Power exponent γ as a function of the polymerization rate ϕ. Adapted from Chaieb *et al.* [25]. Horizontal lines correspond to the data extracted from our NPRG computations: $\gamma_5 = 2.725(2)$, $\gamma_c = 2.510(2)$ and $\gamma_4 = 2.151(3)$.

V. CONCLUSION

The conclusion of our work is fourfold. First, we have shown that the longstanding problem of the wrinkling transition taking place in partially polymerized lipid membranes is both qualitatively and quantitatively

clarified by means of the NPRG approach used in [39]. Second, reciprocally, this agreement validates the NPRG approach to disordered polymerized and, in particular, consolidates the prediction of the existence of three non-trivial fixed points in the RG flow of the model (1), in contradiction with all previous works. At the formal level this situation raises the question of the origin of the mismatch between the NPRG approach and the previous ones: the weak-coupling approach around $D = 4$ performed by Morse *et al.* [57, 58] and the self-consistent screening approximation used by Radzihovsky and Le Doussal [30, 38]. Third, as the three different kinds of scaling behaviors predicted in [39] are associated with fixed points or RG flow, they are universal and should be observed in a large class of defective materials able to display curvature disorder [68]. This is in particular

the case of defective graphene, whose sp^2-hybridized carbon structure can reorganize into a non-hexagonal structure displaying nonvanishing curvature. Fourth, and finally, the glassy graphene configurations observed during the vacancy-amorphization process have been shown to display a rough, static, wrinkled structure with reduced thermal fluctuations with respect to their purely crystalline counterpart and exhibit a root mean squared roughness increasing with vacancy concentration indicating a change in the macroscopic morphological/shape structure of defective graphene sheets [20, 22]. It would be of considerable interest to see if this transition can be moved closer to the wrinkling transition observed in partially polymerized membranes.

* Electronic address: coquand@lptmc.jussieu.fr
† Electronic address: essafi@lptmc.jussieu.fr
‡ Electronic address: kownacki@u-cergy.fr
§ Electronic address: mouhanna@lptmc.jussieu.fr

[1] K. S. Novoselov, A. K. Geim, S. V. Morozov, D. Jiang, Y. Zhang, S. V. Dubonos, I. V. Gregorieva, and A. A. Firsov, Science **306**, 666 (2004).
[2] K. S. Novoselov, A. K. Geim, S. V. Morozov, D. Jiang, M. I. Katsnelson, I. V. Gregorieva, S. V. Dubonos, and A. A. Firsov, Nature **438**, 197 (2005).
[3] A. H. Castro Neto, F. Guinea, N. M. R. Peres, K. S. Novoselov, and A. K. Geim, Rev. Mod. Phys. **81**, 109 (2009).
[4] M. I. Katsnelson, *Graphene: Carbon in Two dimensions* (Cambridge University Press, Cambridge, 2012).
[5] B. Amorim, A. Cortijo, F. de Juan, A. G. Grushin, F. Guinea, A. Gutti?rez-Rubio, H. Ochoa, V. Parente, R. Roldán, P. San-José, J. Schiefele, M. Sturla, and M. A. H. Vozmediano, Phys. Rep. **617**, 1 (2016).
[6] D. Akinwande, C. J. Brennan, J. Scott Bunch, P. Egberts, J. R. Felts, H. Gao, R. Huang, J.S. Kim, T. Li, Y. Li, K. M. Liechti, N. Lu, H.S. Park, E. J. Reed, P. Wang, B.I. Yakobson T. Zhang, Y.W. Zhang, Y. Zhou and Y. Zhu, Extreme Mech. Lett. **13**, 42 (2017).
[7] F. Banhart, J. Kotakoski, and A. Krasheninnikov, ACS Nano **5**, 26 (2011).
[8] L. Liu, M. Qing, Y. Wang, and S. Chen, J. Mater. Sci. Technol. **31**, 599 (2015).
[9] G. Yang, L. Li, W. B. Lee and M.C. Ng, Sci. Technol. Adv. Mater. **19** (2018).
[10] B. Ni, T. Zhang, J. Li, X. Li and H. Gao, *Handbook of Graphene* (Scrivener Publishing LLC, 2019), p. I.
[11] G. López-Polin, C. Gómez-Navarro, V. Parente, F. Guinea, M. I. Katsnelson, F. P?rez-Murano and J.

[12] Gómez-Herrero, Nat. Phys. **11**, 26 (2014).
[12] W. Y. W. Tian, W. Li and X. Liu, Micromachines **8**, 163 (2017).
[13] W.-J. Joo *et al*, Sci. Adv. **3**, e1601821 (2017).
[14] J. Kotakoski, A.V. Krasheninnikov, U. Kaiser and J.C. Meyer, Phys. Rev. Lett. **106**, 105505 (2011).
[15] F.R. Eder, J. Kotakoski, U. Kaiser and J.C. Meyer, Scientific Reports **4**, 4060 (2014).
[16] C.-T. Pan, J.A. Hinks, Q.M. Ramasse, G. Greaves, U. Bangert, S.E. Donnelly and S.J. Haigh, Scientific Reports **4**, 6334 (2014).
[17] J. Kotakoski *et al.*, Nano Lett **15**, 5944 (2015).
[18] Z. Li and F. Chen, Appl. Phys. Rev. **4**, 011103 (2017).
[19] M. Schleberger and J. Kotakoski, Materials **11**, 1885 (2018).
[20] A. R. C. Carpenter and D. Maroudas, Appl. Phys. Lett. **100**, 203105 (2012).
[21] M. W. A. Kumar and M. Thorpe, J. Phy.: Condens. Matter **24**, 485003 (2012).
[22] R. Ravinder, R. Kumar, M. Agarwal and N.M. Krishnan, Scientific Reports **9**, 4517 (2019).
[23] W. Zachariasen, Journ. Am. Chem. Soc. **54**, 3841 (1932).
[24] D. M. C. Carpenter and A. Ramasubramanian, Appl. Phys. Lett. **103**, 013102 (2013).
[25] S. Chaieb, V.K. Natrajan, and A. A. El-rahman, Phys. Rev. Lett. **96**, 078101 (2006).
[26] M. Mutz, D. Bensimon, and M. J. Brienne, Phys. Rev. Lett. **67**, 923 (1991).
[27] D. Bensimon, D. Mukamel, and L. Peliti, Europhys. Lett. **18**, 269 (1992).
[28] D. R. Nelson and L. Radzihovsky, Europhys. Lett. **16**, 79 (1991).
[29] L. Radzihovsky and D. R. Nelson, Phys. Rev. A **44**, 3525 (1991).
[30] L. Radzihovsky and P. Le Doussal, J. Phys. I France **2**, 599 (1992).
[31] D. Bensimon, M. Mutz, and T. Gulik, Physica A **194**,

190 (1993).

[32] R. Attal, S. Chaieb, and D. Bensimon, Phys. Rev. E **48**, 2232 (1993).

[33] Y. Park and C. Kwon, Phys. Rev. E **54**, 3032 (1996).

[34] S. Mori, Phys. Rev. E **54**, 338 (1996).

[35] A. Benyoussef, D. Dohmi, A. E. Kenz, and L. Peliti, Eur. Phys. J. B **6**, 503 (1998).

[36] P. Le Doussal and L. Radzihovsky, Phys. Rev. B **48**, 3548 (1993).

[37] S. Mori and M. Wadati, Phys. Lett. A **185**, 206 (1994).

[38] P. Le Doussal and L. Radzihovsky, Annals Phys. **392**, 340 (2018).

[39] O. Coquand, K. Essafi, J.-P. Kownacki, and D. Mouhanna, Phys. Rev E **97**, 030102 (2018).

[40] E. Sackman, P. Eggl, C. Fahn, H. Bader, H.Ringdorf and M. Schollmeier, Ber. Bunsenges. Phys. Chem. **89**, 1198 (1985).

[41] S. Chaieb, S. Málková, and J. Lal, J. Theor. Biol. **251**, 60 (2008).

[42] S. Chaieb, Scientific Reports **4**, 3699 (2013).

[43] S. Chaieb, Scientific Reports **4**, 7347 (2014).

[44] D. R. Nelson and L. Peliti, J. Phys. (Paris) **48**, 1085 (1987).

[45] D. R. Nelson, T. Piran, and S. Weinberg, eds., *Proceedings of the Fifth Jerusalem Winter School for Theoretical Physics* (World Scientific, Singapore, 2004), 2nd ed.

[46] M. J. Bowick and A. Travesset, Phys. Rep. **344**, 255 (2001).

[47] J. A. Aronovitz and T. C. Lubensky, Phys. Rev. Lett. **60**, 2634 (1988).

[48] E. Guitter, F. David, S. Leibler, and L. Peliti, J. Phys. (Paris) **50**, 1787 (1989).

[49] P. Le Doussal and L. Radzihovsky, Phys. Rev. Lett. **69**, 1209 (1992).

[50] J.-P. Kownacki and D. Mouhanna, Phys. Rev. E **79**, 040101 (2009).

[51] D. Gazit, Phys. Rev. E **80**, 041117 (2009).

[52] F. L. Braghin and N. Hasselmann, Phys. Rev. B **82**, 035407 (2010).

[53] K. V. Zakharchenko, R. Roldán, A. Fasolino and M. I. Katsnelson, Phys. Rev. B **82**, 125435 (2010).

[54] R. Roldán, A. Fasolino, K. V. Zakharchenko, and M. I. Katsnelson, Phys. Rev. B **83**, 174104 (2011).

[55] N. Hasselmann and F. L. Braghin, Phys. Rev. E **83**, 031137 (2011).

[56] S. F. Edwards and P. W. Anderson, J. Phys. F: Met. Phys. **5**, 965 (1975).

[57] D. C. Morse, T. C. Lubensky and G. S. Grest, Phys. Rev. A **45**, R2151 (1992).

[58] D. C. Morse and T. C. Lubensky, Phys. Rev. A **46**, 1751 (1992).

[59] K. Essafi, J.-P. Kownacki, and D. Mouhanna, Phys. Rev. Lett. **106**, 128102 (2011).

[60] K. Essafi, J.-P. Kownacki, and D. Mouhanna, Phys. Rev. E **89**, 042101 (2014).

[61] O. Coquand and D. Mouhanna, Phys. Rev. E **94**, 032125 (2016).

[62] A. Locatelli, K. R. Knox, D. Cvetko, T. O. Mentes, M. A. Nino, S. Wang, M. B. Yilmaz, P. Kim, R. M. Osgood Jr, A. Morgante, ACS Nano **4**, 4879 (2010).

[63] L. Canet, B. Delamotte, D. Mouhanna, and J. Vidal, Phys. Rev. D **67**, 065004 (2003).

[64] The notation η is employed in [25] in place of γ while η is used here to indicate the anomalous dimension.

[65] With a stretching factor (noted ζ in [39] that should not be confused with the roughness exponent) taken equal to one.

[66] See [38] for a careful discussion about the scaling behavior of the correlation functions.

[67] Error bars have been obtained by using three families of cut-off functions $\widetilde{R}_k(q) = \alpha Z_k(q^4 - k^4)\theta(q^2 - k^2)$, $\widetilde{R}_k(q) = \alpha Z_k q^4/(\exp(q^4/k^4) - 1)$ and $\widetilde{R}_k(q) = \alpha Z_k k^4 \exp(-q^4/k^4)$ that are used to separate high and low momenta modes within the RG process (see [39]). Above, α is a free parameter used to investigate the cut-off dependence of physical quantities and allows, in particular, to optimize each cut-off function inside its family, *i.e.* to find stationary values of these quantities, see for instance [63]. Error bars follow from the comparison between the results corresponding to different optimized cut-off functions.

[68] As observed for the first time by Morse *et al.* [57, 58], a curvature disorder generates metric disorder.